American Journal of Nanomaterials, 2023, Vol. 11, No. 1, 41-50
Available online at http://pubs.sciepub.com/ajn/11/1/3
Published by Science and Education Publishing
DOI:10.12691/ajn-11-1-3

Review of Recent Advances of GaN Nanostructured Based Devices

M. Abdulrahman, A. Khalil, Ahmed M. Nahhas*

Department of Electrical Engineering, Faculty of Engineering and Islamic Architecture,
Umm Al Qura University, Makkah, Saudi Arabia
*Corresponding author: anahhas@hotmail.com

Received December 14, 2022; Revised January 22, 2023; Accepted February 08, 2023

Abstract This paper is intended to provide an overview of recent advances of GaN based nanostructured materials and devices. Because of its unique electrical, optical, and structural properties, GaN has sparked significant interest in the field of wide bandgap semiconductor research. Because of its higher surface-to-volume ratio than thin films, GaN nanostructured material offers numerous advantages for nanodevices. The ability of GaN nanostructured material to absorb ultraviolet (UV) radiation is invaluable in many optical applications. GaN nanostructured-based devices have recently received a lot of interest due to their numerous potential uses. GaN has been employed as a nanomaterial in a variety of devices, including UV photodetectors, light-emitting diodes, solar cells, and transistors. The most current developments in GaN-based devices are presented and reviewed. The performance of many device architectures demonstrated on GaN is presented. The structural, electrical, and optical characteristics are also discussed.

Keywords: *gallium nitride (GaN), nanostructured, light emitting diodes, nanowires, ultraviolet, doping*

Cite This Article: M. Abdulrahman, A. Khalil, and Ahmed M. Nahhas, "Review of Recent Advances of GaN Nanostructured Based Devices." *American Journal of Nanomaterials*, vol. 11, no. 1 (2023): 41-50. doi: 10.12691/ajn-11-1-3.

1. Introduction

The group III-Nitride semiconductor materials have attracted a lot of interest for new generation of optoelectronic devices [1]. The advantage with these materials is the flexible bandgap varying from 0.7 to 6 eV hence covering an ultra-broad spectrum, from deep ultraviolet up to near infrared [1], which has been employed in various applications such as optoelectronic devices, electronic devices, biosensors, chemical sensors and so on [2]. Solar cells based on nitride materials have readily been investigated for terrestrial and space-based applications [1]. Transistors performance for high power electronics, ground-based communications and biological agent detection devices has been enhanced [1]. Major efforts have been dedicated to technological fabrication to achieve efficient emitters and detectors [1]. Recent progress has demonstrated cutting edge results in high-speed data rate connectivity and integrated circuits [1]. Imaging sensors on high-speed electronics have been implemented founded on their sensitive applications in security screening [1].

GaN as a member of group III-nitride family has become a revolutionary material owing to its electronic and optical properties. The direct, flexible, and wide bandgap makes GaN materiel a key candidate for achieving high frequency, large bandwidth, high power, and efficiency devices. GaN based detectors are in particular suitable for full color display, high density information storage, and UV communication links [1].

GaN has a direct and wide band gap of 3.4 eV at room temperature, it is quite robust [3]. Other group III elements like Aluminum (Al) and Indium (In) can be alloyed with Ga to tune the bandgap of III-nitrides from 0.8 eV to 6 eV [3]. Moreover, it possesses high electron mobility, high heat capacity and high breakdown voltage [3], which makes it suitable to be used for sensors, for high power electronic devices such as field effect transistor (FET) and for optoelectronic devices such as light emitting diode (LED) [1]. The optical properties of GaN nanostructured are of great current interest because of the potential application in solid state lighting [1]. In n-type GaN, an UV peak at approximately 3.42 eV usually dominates the photoluminescence spectrum [1]. The blue luminescence at 2.7 to 3 eV peak energy has been extensively studied; this peak dominates due to optically active defects and impurities [1]. On the other hand, such defects can be destructive in a device. A well-engineered inorganic nanoparticle approach offers many advantages [1]. Meanwhile, in nanostructures having a large specific area, the surface states effect became significant in influencing the carrier recombination mechanism [1].

2. GaN Nanostructured Materials Doping

Nanostructures are typically created using either a bottom-up or a top-down technique. Metal-organic chemical vapor deposition (MOCVD), molecular beam epitaxy (MBE), the vapor-liquid-solid (VLS), laser-assisted catalytic growth (LCG), and the ion-etching reaction have all been used to create well-aligned GaN nanostructures [4,5,6]. GaN nanostructured material is better for nanodevices than thin films because it has a higher ratio of surface to volume. GaN nanostructured material can absorb UV light and is very useful in a wide range of optical applications [7]. GaN nanostructures come in many different shapes, such as nanowires, nanoparticles, nanobelts, nanorings, nanotubes, nanodots, and nanorods [8]. GaN nanoparticles have been getting a lot of attention from scientists and engineers over the past few years. Quantum confinement of electrons in nanoparticles gives them useful electronic properties that make them useful in many GaN applications [9].

Doping GaN is crucial for a wide variety of device architectures. GaN doping has been accomplished in a few different ways [10]. For GaN-based high-power devices, reaching levels of performance close to their theoretical limits has been hampered by the difficulty of regulating n-type or p-type conduction using the ion implantation procedure [11]. Activation rates of 86% and roughly 100% have been reported in prior research on the n-type conduction of GaN through silicon ion implantation, after annealing at 1250 and 1400 °C, respectively [12]. GaN's surface is severely degraded during high-temperature annealing owing to breakdown [13]. But picking the right protective layer that doesn't change and can be easily removed after annealing at temperatures above 1200 degrees Celsius is tricky [13]. Therefore, it is crucial to get the high activation rate at a lower temperature. However, because of the higher temperature annealing required for electrical activation, preserving the surface during Mg ion implantation for *p*-type conductivity is much more difficult [14]. Mg on the Ga site (MgGa) has a formation energy in the valence band that is around 1 eV higher than that of SiGa at the Fermi level near the conduction band, which may account for the difference in annealing temperatures between the two conduction types [15]. In general, efficiently doping GaN to the *p*-type is difficult. Even though high-quality *p*-type GaN has been realized, the activation efficiency of Mg atoms is still in the single-digit percentage range [16]. While there has been some discussion of *p*-type doping of GaN using ion implantation and diffusion, publications on these and other doping methods commonly used in semiconductor fabrication have been uncommon [17]. Changing the concentration profile of implanted Mg was discovered via an investigation into the thermal stability and redistribution of implanted dopants in GaN. Indeed, high temperature annealing of GaN after implantation is required for Mg redistribution and activation as well as lattice recovery [18]. This annealing is commonly performed between 1100 and 1400°C [19]. However, nitrogen desorption causes significant surface damage to GaN during annealing at temperatures exceeding 800-900°C [20]. This extreme sensitivity to post-implantation heat treatments means that a cap layer must be used to shield the GaN surface and prevent nitrogen desorption [21].

As of late, carbon doping of GaN has also been achieved. Carbon may be deliberately doped onto GaN via a hydrocarbon precursor method [22]. In terms of the voltage capabilities of the device, the extrinsic carbon doping results in superior dynamic qualities [23]. Optimal solutions for effective dc-dc conversion may be found in devices like GaN on silicon (Si) devices [24]. For a long time now, they've also been clearly superior to their Si counterparts in terms of handling high voltage operation at a high switching frequency [25]. The most frequent technique for creating extremely resistive GaN buffers is carbon compensatory doping, which is employed due to the necessity for high blocking voltage [26]. High dynamic on resistance and slowly recovering current collapse are just two of the major drawbacks of carbon-doped GaN heterostructure field effect transistors [27]. Incorporation of carbon from the metal organic precursor during growth is the classic method for achieving carbon doping [28]. High carbon concentrations required a low growth temperature, pressure, and V/III ratio [29]. The result was decreased blocking voltages and reduced electron mobility in the channel, as a result of a combination of poor crystal quality and a high dislocation density [30]. Incorporating carbon while preserving growth settings suited for crystal quality through extrinsic carbon doping of GaN buffers has been gaining traction of late [31].

GaN is a desirable alternative to InGaN for red LEDs due to the InN-rich alloy's surprisingly poor luminous efficiency [32]. GaN demonstrates self-compensation, where acceptor doping is neutralized by native donors, which is energetically advantageous for the crystal [33]. The thermodynamic study of the defect chemistry in GaN:Mg crystals indicates that a MgGa acceptor-controlled p-type can only be obtained at N2 pressures greater than 104 MPa [34]. Due to donor recombination, Mg-doped GaN films exhibit wide emission bands in the region of 2.8–3.3 eV [34]. Mn has limited solubility in gallium and its group V compounds; hence, phase separation occurs during the development of GaMnAs when Mn concentrations greater than 5% are used [34]. Pulsed laser deposition (PLD) may be used to produce thin films from multicomponent targets and permits easy control of Mn concentrations [34].

3. GaN Based Nanostructured Devices

3.1. Sensors

The GaN nanostructures properties effect the performance of the gas sensors. Ashfaque et al. studied reported on the GaN nanostructures-based sensors for the detection of various gases [3] including alcohols (R-OH), methane (CH_4), benzene and its derivatives, nitric oxide (NO), nitrogen dioxide (NO_2), sulfur-dioxide (SO_2), ammonia (NH_3), hydrogen sulfide (H_2S), and carbon dioxide (CO_2) [3]. In that work, the sensing performance of GaN nanostructure-based sensors devices have been described, a unique measure called the most essential sensing performance data, including the limit of detection, response/recovery time, and operating temperature, have been compiled and tabulated for each of the numerous types of sensors to give

a comprehensive performance comparison [3]. For the product of reaction time and limit of detection has been devised [35]. It was discovered that the InGaN/GaN NW-based sensor has greater overall sensing capability for the detection of H_2 gas [36]. On the other hand, the GaN/(TiO_2–Pt) nanowire-nanoclusters

(NWNCs)-based sensor is superior for the detection of ethanol [37]. TNT sensing is another application that works quite well with the GaN/TiO_2 NWNC-based sensor [38]. In another article included a summary of initial primary research that was based on density-functional theory (DFT), looked at the interaction between gas molecules and GaN [39]. In addition, the use of machine learning techniques to nanostructured GaN sensors and sensor arrays has been investigated and examined [40]. The last topic of discussion was the gas sensing method on GaN nanostructure-based sensors operating at ambient temperature [41]. Figure 1 shows the sensors based on GaN nanostructures to detect H_2, alcohols, and additional gases, and that study also compares their reaction times and sensitivity limits.

3.2. GaN Based LEDs

Significant progress has recently been made on group III-nitride nanostructure-based LEDs across the entire color spectrum, from DUV to NIR, by modulating the bandgap of Al(Ga/In)N nanostructures. This has resulted in several exciting new developments [42]. LEDs based on group III nitride nanostructures typically used nitride p-n homo- and heterojunctions, *n*-nitride/*p*-semiconductor, and *n*-semiconductor/*p*-nitride. In this part, the current developments that have taken place in the field of group III-nitride nanostructures for LEDs with color-adjustable emission are discussed [43].

3.2.1. Ultraviolet LEDs

Since the original demonstration of nanostructured GaN LEDs employing two single NWs, comprising a Si-doped *n*-GaN nanowire and a Mg-doped *p*-GaN NW, there has been increased interest in tuneable light emission sources based on 1D nanostructures embedded with p-n junctions [44]. GaN nanowires p-n junction and *n*-ZnO/*p*-GaN heterojunction nanowire LEDs are shown in Figure 2 [45]. Mg doping led to the formation of *p*-GaN nanowires from N vacancies and/or O impurities [45]. The rectifying I-V curve of a p-n GaN nanowire-based LED is shown in Figure 3(a). Forward biasing the p-n junction of a GaN nanowire LED causes light emission. As shown in Figure 3(b), the emission peak of GaN nanowire p-n junction LEDs is 3.179 eV (390 nm) regardless of current injection [46]. The turn-on voltage and rectification ratio for the single *n*-ZnO/*p*-AlGaN NW-based LED device are shown in Figure 3(c) as 2 V and 4:1, respectively [47]. Band-filling increased EL significantly as current increased [48]. As demonstrated in Figure 3(d), when the injection currents are between 1 and 4 A, the monopeak remains at 394 nm, while the EL peak shifts to 400 nm at 5 A [49]. At modest injection currents, the *p*-AlGaN side radially recombined the injected carriers at 394 nm [51]. When the current was high enough, holes could be injected into the *n*-ZnO side, resulting in radiative recombination at the band edge at 400 nm [52].

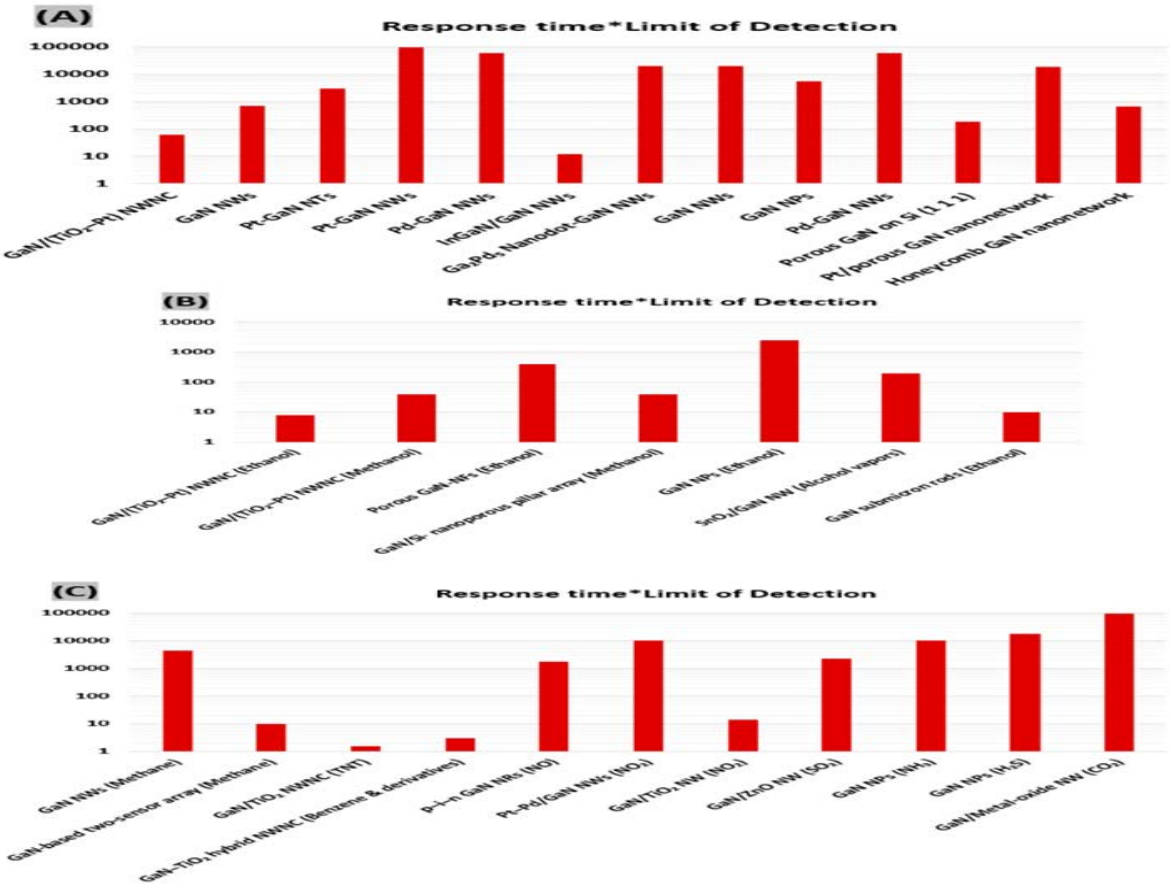

Figure 1. Comparison of the product of response time and limit of detection value among previously reported GaN nanostructures-based sensors for (A) H_2, (B) alcohols, and (C) other gases [3]

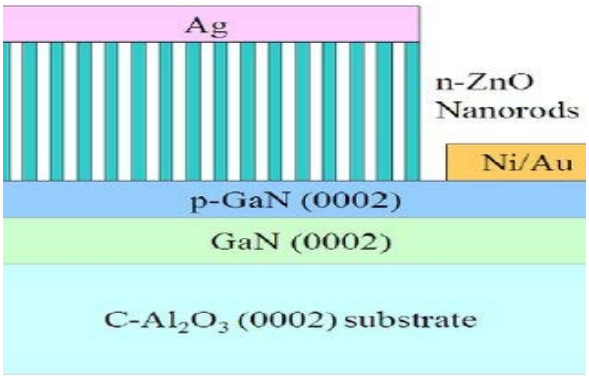

Figure 2. An illustration of the investigated LED structure, which consists of *n*-ZnO nanorods grown vertically atop *p*-type GaN sheets [45]

Mi's team created a practically defect-free [53].

AlGaN tunnel junon (TJ) nanowire [53]. As shown in Figure 4(a) and Figure 4(b), the EL emission peak of the AlGaN nanowire LED with the n+-GaN/Al/p+ efficiency of 0.012% [53]. With an Al-rich AlGaN shell surrounding the AlGaN nanowires with TJ, as shown in Figure 4(c)-(d), the core-shell nanowire heterostructure enabled efficient carrier confinement in the nanowire LED active area and suppressed nonradiative surface recombination [53]. The creation of double heterostructures was attributed to -AlGaN TJ is centered at 242 nm, demonstrating greater EL emission compared to the AlGaN NW-LED without TJ due to enhanced electrical quantum performance [54]. The EL intensity was multiplied by 400, approximately. The highest output power of unpackaged TJ UV LEDs producing at 242 nm was measured to be 0.37 mW, with a maximum external a very narrow emission peak at 275 nm and a lack of considerable peak-shifting with increased injection current [55]. The unpackaged Al TJ DUV LED had an output power of more than 8 mW and a peak EQE of 0.4%, which were about one to two orders of magnitude greater than their AlGaN nanowire devices [56]. Due to the integration of Al TJ and the deletion of the resistive and absorptive *p*-GaN contact layer, it is claimed that the increased LED performance is a result of greatly improved hole transport and injection into the device active area [57].cti

Mg has been extensively utilized as a *p*-type dopant in GaN; however, AlN presents substantial hurdles because of its unusually high ionization energy (600 meV) [58]. Furthermore, the presence of free holes in Mg-doped AlGaN is strongly counterbalanced by the formation of large native defects and impurity incorporation during the epitaxy of highly mismatched lattice AlGaN epilayers [59]. To overcome the inherent disadvantage of low *p*-type conductivity in Al-rich AlGaN for deep ultraviolet (DUV) LEDs, hexagonal boron nitride (h-BN) may be an ideal candidate due to its large bandgap, near-zero polarization field, small ionization energy (150 meV), and especially the unusual propensity for *p*-type doping in the presence of B vacancies [60]. Using h-BN, Maity et al. [61] established a unique h-BN/AlGaN p-n junction to solve *p*-type doping difficulties in Al-rich AlGaN [61]. In addition, Yang et al. reported that h-BN can function as a highly conductive, DUV-transparent electrode in the Mg-free nanowire-array-based Al(Ga)N/h-BN LED and that the hole concentration is as high as 1020 cm^3 at room temperature, which is 10 orders of magnitude higher than that of previously reported Mg-doped AlN epilayers [62].

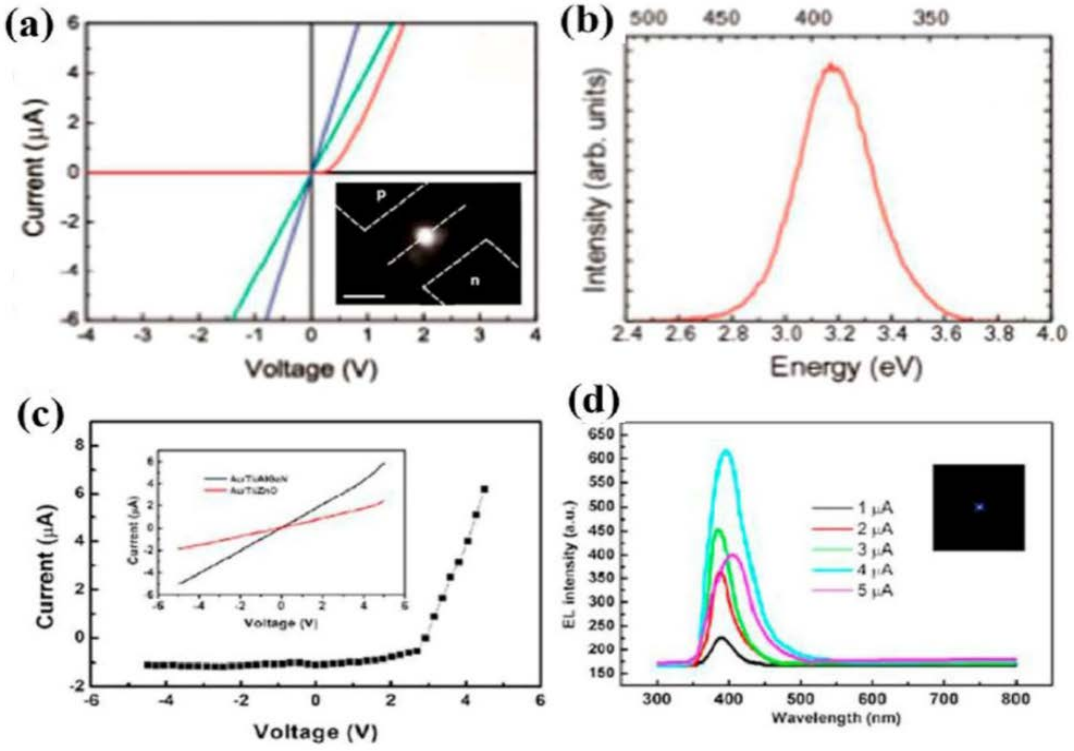

Figure 3. (a) I-V behaviour of n-n (blue), p-p (green), and p-n (red) junctions; (b) the corresponding CL spectrum; (c) I-V curves of (e) RT EL spectra of a single *n*-ZnO/*p*-AlGaN heterojunction nanowire under various injection currents, with a CCD picture of the device under a 4 A injection current in inset [46]

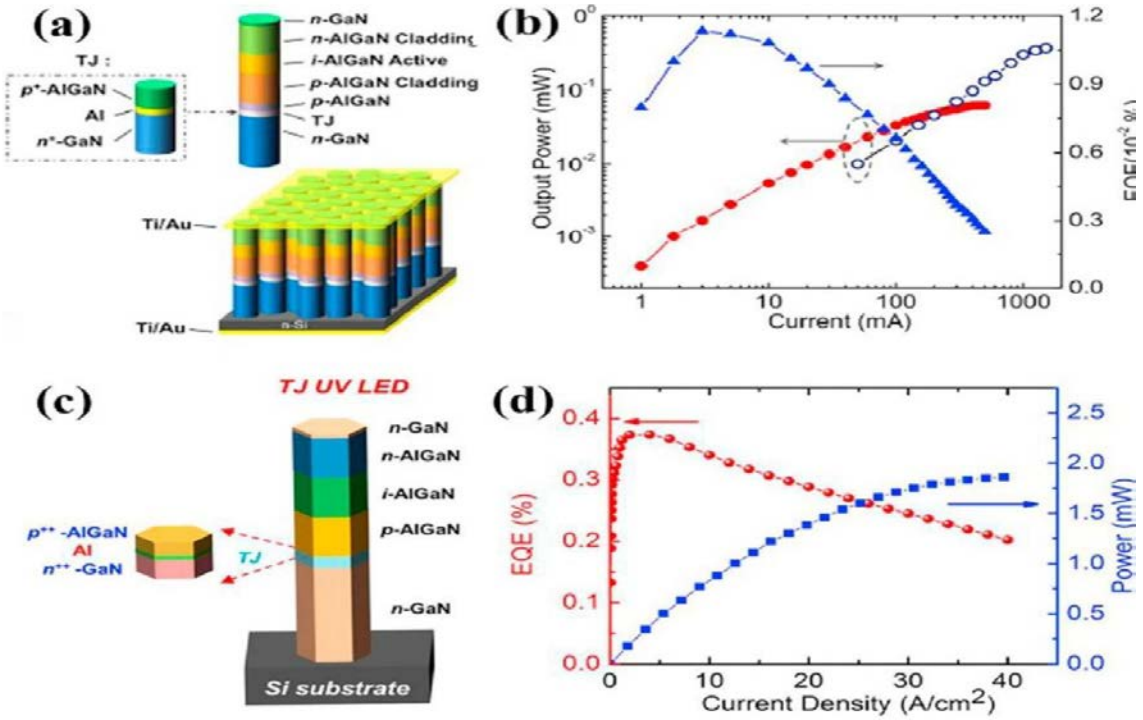

Figure 4. (a)-(b) Schematic of the AlGaN nanowire TJ UV LED structure (a), and RT output power and EQE of TJ UV LEDs (b); (c)-(d) Schematic diagram of an Al TJ AlGaN UV LED (c), and RT output power and EQE of TJ UV LEDs (d) [42]

3.2.2. Visible LEDs

3.2.2.1. Single-color LEDs.

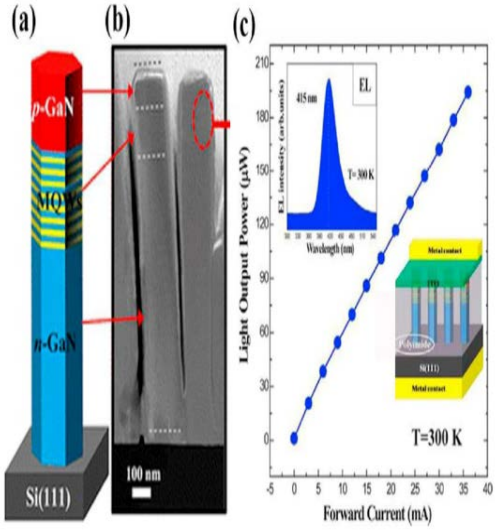

Figure 5. (a) Light output power of nanowire LED, as a function of current, top-left, and bottom-right showing the EL and schematic of the LED structure, respectively; (b) low and high-magnification TEM images of the nanowire; (c) light output power of nanowire LED, as a function of current [42]

By alloying the binary material, the bandgap of Group III-nitride nanostructures may be tuned across a broad range in the visible light spectrum, making them very promising for use in a variety of color LED applications [63]. The introduction of trace quantities of Mg and Si, respectively, enables the creation of an epitaxial p-n homojunction, resulting in the efficient radiative recombination of electrons and holes [64]. On the basis of group III-nitride nanostructures, it is possible to create LEDs of different colors [65]. Liang et al. have described axial group-III-nitride nanowire LEDs [66]. Subsequently, a great deal of study was devoted to the investigation of LEDs with axial III nitride nanostructures that emit light of different colors and have a high efficiency [66]. Lu et al. observed a single peak emission of 415 nm from a p-GaN/InxGa1-xN/GaN MQW/n-GaN nanowire LED, as shown in Figure 5(a)-(b)-(c) [67]. By adjusting the number of MQW pairings using the MOCVD process, the MQW structures precisely regulated in content were adjusted [68]. The output power rose linearly with increasing current due to the uniform and defect-free InxGa1-xN/GaN MQW nanowire structure [68].

3.2.2.2. Color Tunable LEDs.

Color-tuneable LEDs with chosen CCT and CRI enable displays, smart illumination, and real-time cell identification. Phosphor-free, high-efficiency tuneable-light LEDs were designed to address phosphor LEDs' poor CRI and Stokes fluorescence loss [69]. Color-tunable LEDs with very tiny size, low power consumption, and good CRI may be possible by directly integrating RGB LEDs on a chip [70]. Much work has gone into making color-tunable III-nitride nanostructure LEDs [71]. The following categories summarize recent III-nitride nanostructure LED tuneable color emission studies: Tuning the In composition in pure InGaN nanowires or (Al, In) GaN/GaN 1D MQW/MQD heterostructures; designing special heterostructures and measuring device performance under different injection currents/applied voltages/current injection modes; and integrating the different areas with tunable color emission directly on a single chip [72].Meier et al. created a single *n*-GaN/InxGa1-xN/GaN/*p*-AlGaN/*p*-GaN core/multishell (CMS) NW LED, as shown in Figure 6(a)-(b) [73]. Discrete connections were created to the *n*-type core and p-type shell of the isolated single NW device. InxGa1-xN NWs with x of 0.01, 0.1, 0.2, 0.25, and 0.35, respectively,

were able to produce EL emissions at 367, 412, 459, 510, and 577 nm. As shown in Figure 6(c)(d), Alfaraj et al. successfully implemented the tuneable emission using InGaN NW LEDs [74]. By modulating the VT of the In and Ga sources during the CVD development, the In composition of InGaN NWs produced on *p*-GaN/Al_2O_3 substrates was controlled in the range of 0.06–0.43 [75]. The EL emission peaks were adjusted from 435 nm to 575 nm, i.e., from blue to orange hues, with increasing In concentration due to the tunable bandgap of InxGa1-xN NWs [76].

Robin et al. [77] demonstrated visible-color tuneable LEDs using InGaN thin-film integrated in position-controlled GaN nanowire arrays [77]. Anisotropic MQWs with varying QW thickness and composition were produced on different facets of *n*-GaN nanowires during the heteroepitaxial overgrowth of the InGaN/GaN MQW layers [78]. With increasing bias voltage, the EL spectra of nanostructured LEDs exhibited a continuous peak shift from red to blue emission [78]. Both the anisotropic MQW layers generated on the multifunctional GaN nanowires and the progressive change in electric field distributions in nanowire-embedded thin-film structures upon altering electric bias contributed to the highly adjustable emission color of these nanowire-embedded thin film LEDs [78]. Using the same method, they also showed the ability to adjust the emission color of InGaN/GaN microdonut array LEDs from green to blue [78].

3.2.2.3. White Light LEDs

InGaN nanostructures emit virtually all visible light efficiently [79]. Phosphor-free white light LEDs use core-shell heterostructures and quantum in 1D GaN nanostructures [80]. Priante et al. [81] demonstrated axial nanowire LED heterostructures with self-organized core-shell InGaN/AlGaN dots in *p*-GaN:Mg/*n*-GaN:Si nanowire arrays [81]. Due to the many AlGaN shell and barrier layers, the InGaN/AlGaN dot-in-a-wire core-shell LED active area has better 3D carrier confinement [82]. The AlGaN barriers surrounded and capped the ten InGaN dots, forming an Al-rich shell at the nanowire sidewall [83]. The dot-in-a-wire core-shell LED output EL spectra were steady and almost independent of injection currents [84]. The LED's CCT was 4450 K and its CRI was 95. Embedding InGaN quantum dots/nano disks in defect-free 1D GaN nanostructures is an efficient method for producing phosphor-free white light LEDs [85]. The nanowire LED emitted a bright white light. Moreover, the CIE chromaticity coordinates of the *p*-type doped LED hardly changed as the injection current increased [86]. Comparing the RT IQE of undoped and *p*-type doped LEDs, the IQE of *p*-type doping (56.8%) was almost 50% higher than that of undoping (36.8%), which was sufficient for phosphor-free white LEDs [87]. As a result, group III-nitride nanostructures provide an alternate strategy for increasing lifespan and improving light quality [87].

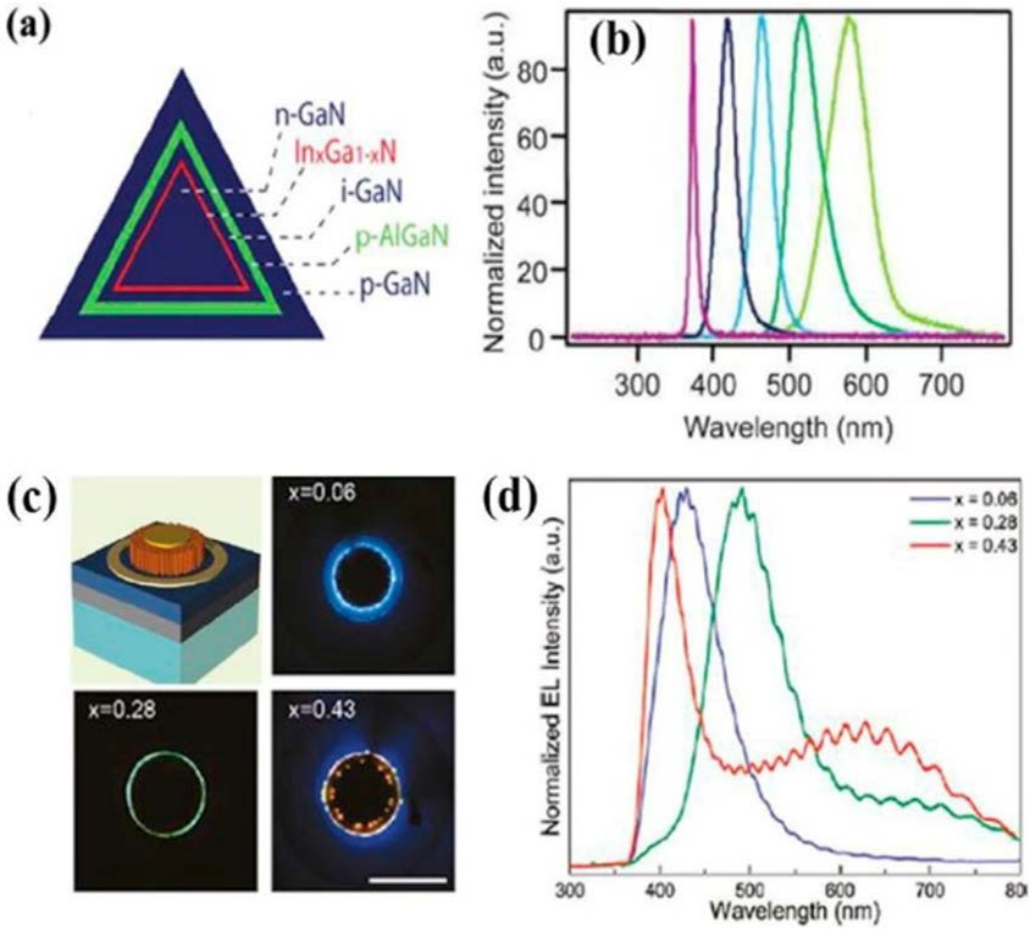

Figure 6. (a) A diagram of a CMS NW, which is composed of *n*-GaN, InxGa1-xN, GaN, *p*-AlGaN, and *p*-GaN; (b) normalized EL spectra of the LEDs. Panel (c) schematic and OM images of the InGaN nanowire LED device under forward bias (V = 19, 9, and 11 V for x = 0.06, 0.28, and 0.43, respectively); panel (d) normalized EL spectra of each device in panel (c) [42]

3.2.3. Micro-LEDs

Micro-LEDs (-LED), with a micro-size of 1030 m, are now considered the ultimate display technology because of their inherent high brightness, high contrast ratio, quick response speed, extended lifespan, power-saving qualities, and ability to be operated across a broad temperature range [88]. Since the first current injection of -LED (12 m) based on *p*-GaN/InGaN/*n*-GaN QWs was reported, a great deal of focus has been placed on the advancement of -LED, with promising products appearing in areas such as wearable displays for high-speed3D/AR/VR display applications, high-brightness/contrast large flat-panel displays and TVs, light sources for the neural interface, and optogenetics [88]. For instance, Jiang et al. reported the use of InGaN/GaN-based nanocolumns (NC) to create multicolor (red, green, blue, and yellow; RGBY) LED pixels with 5 m^2 emission [90].

3.3. Photodetectors

Because the direct bandgap energies of GaN materials are different, their 1D nanostructures can be used to make photodetectors that work from the deep ultraviolet to the near infrared.

3.3.1. Photodetectors are Based on Undoped GaN Nanostructures

Nanowires has been widely studied in recent years [90]. Yin et al. [91] reported the dark and illuminated electrical transport performance of a single GaN nanowisker in 2021. Due to the presence of depletion space charge layers, the diameter of the nanowires determined the photocurrent of the GaN nanowires PD device [92]. The accelerated recombination process inside nanowires with short diameters screened the depletion electric field, resulting in a reduction in photocurrent [93]. Nonetheless, the photocurrent exhibited a minor effect on the diameter, since the vast bulk volume remained unconsumed [94]. Johar et al. [95] developed single nanowire PD based on axial GaN nanowires on patterned Si. With a reaction time of less than 25 ms, the device displayed a high responsivity of up to 10,000 A/W [96].

3.3.2. Photodetectors Based on Doped GaN Nanostructures

Group III-nitride nanostructures with added dopants have been shown to be an efficient method of achieving the necessary optical and electrical features [97]. The efficiency of PDs made from group III-nitride nanostructures might also be improved using this method [98]. Concordel et al. [100], for instance, looked at how *n*-type doping affected the electrical transport performance of GaN nanowires of varying diameters. Under UV light, GaN nanowires with highly doped Si had a much greater photocurrent than nanowires with undoped or mildly doped Si [100]. The photoconductivity performance of Mg doped nonpolar GaN nanowires was reported by Subramani et al. [101]. In the presence of light at 470, 530, and 788 nm wavelengths, the constructed devices had an extremely high on-off ratio of 100 [102].

3.3.3. Photodetectors Based on GaN Homo/Heterostructures

On the basis of III-nitride nanostructures, photodetectors with an active p-n junction have been constructed [103]. When light shines onto the connection, a proportionate reverse current may be observed [104]. Aiello et al. [105] demonstrated GaN quantum disk-based UV photodetectors in a single GaN nanowire. The gadget demonstrated a significant decrease in dark current and an increase in photocurrent Yang et al. [106] described the manufacture and characterization of visible blind photodetectors based on an array of p-i-n junction GaN nanowires, as shown in Figure 7. In moreover, the photocurrent emerged at 3.27 eV and rose by more than two orders of magnitude between 3.3 and 3.4 eV; the ratio of UV to visible photocurrent rejection was 200 [107]. Such visible band detectors found interesting uses in photodetectors with fast speeds [108]. Shen et al. [109] subsequently proved the photocurrent performance of a single axial GaN n-i-n nanowire produced by PAMBE. The photoconductive gain of the device was between 105 and 108, and the UV (350 nm) to visible (450 nm) responsivity ratio was more than 106. Recently, Spies et al. [110] recently revealed the UV photo sensing performance of a single GaN nanowire with AlN/GaN: Ge axial heterostructures. Both the integration of heterostructures and the increase in the number of active nano disks and AlN barriers were shown to reduce the dark current and enhance photosensitivity. In addition, work has been done to enhance the photoconductive performance of III-nitride nanostructure-based PDs by using a variety of materials for the electrodes [111]. The manufacturing and photoconductive capabilities of the PDs utilizing few layer graphene contact to GaN nanowire ensemble were reported by Sarkar et al. [112].

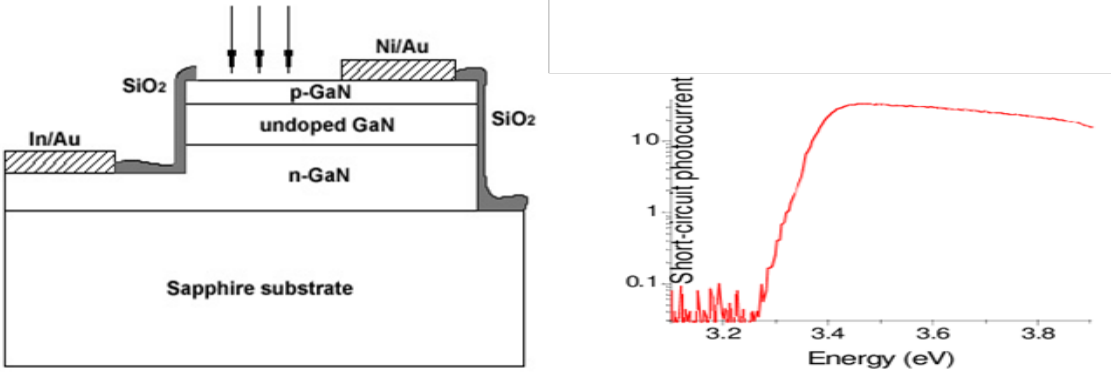

Figure 7. Schematic representation of p-i-n GaN nanowires photodetector and RT photocurrent spectrum under zero applied bias [107]

4. Conclusion

In this review paper, we provide a comprehensive look at the production and properties of GaN nanostructures. GaN has some promises for electrical and photonic devices and encouraging progress has been made in the research phase. Despite this advancement, there are a number of critical challenges that must be addressed before this material can be commercially used for the claimed uses. The extremely successful GaN, which competes for comparable applications, makes the process more challenging. GaN contributes to optical device applications in part owing to the simplicity with which GaN may be generated in nanostructured form. There is still much to study about the mechanisms of GaN-based optical devices.

Although a number of GaN optical devices have been described, there are several difficulties that require additional inquiry and development. These challenges include *p*-type doping; the lack of plausible *p*-type doping hinders the widespread use of optical emitters in GaN. Furthermore, GaN's highly ionic nature, which results in strong electron photon coupling and low heat conductivity, does not bode well for GaN-based electrical systems. Nanostructures appear to be a bit simpler to generate using GaN, but it remains to be seen whether nanostructures in general, as advertised, can actually make inroads in the device field. In terms of nanostructures, GaN nanostructured devices such as nanowires and nanorods offer a path to a new generation of devices; however, a concerted effort is required for GaN nanostructured to be taken seriously for large scale device applications, as well as to achieve high device density with access to individual nanodevices. It is necessary to create reliable ways for assembling and integrating building blocks into circuits.

References

[1] Nahhas, A. M., "A Review of GaN Nanowires Based Sensors," American journal of nanomaterials. 6(1):1-14. (2018).

[2] Khan, A., Rao., M., Qiliang, L. "Recent Advances in Electrochemical Sensors for Detecting Toxic Gases: NO_2, SO_2 and H_2S". *Sensors.;* 19: 905, (2019).

[3] Khan, M. "Gallium nitride (GaN) nanostructures and their gas sensing properties": A review. *Sensors*. 20(14):3889, (2020).

[4] Sun, D., Priante, D., Min, W., Subedi, R., Shakfa, M., Ren, Z., Li, K., Lin, R., Zhao, C., Ng, T., et al. "Graded-Index Separate Confinement Heterostructure AlGaN Nanowires: Toward Ultraviolet Laser Diodes Implementation". ACS Photonics, 5, 3305, (2018).

[5] Huo, Q., Shao, Y., Wu, Y., Zhang, B., Hu, H., Hao, X. "High quality self-separated GaN crystal grown on a novel nano porous template by HVPE". Sci. Rep, 8, 3166, (2018).

[6] Li, P., Zhang, H., Li, H., Zhang, Y., Yao, Y., Palmquist, N., Iza, M., Speck, J., Nakamura, S., DenBaars, S. "Metalorganic chemical vapor deposition grown n-InGaN/n-GaN tunnel junctions for micro-light-emitting diodes with very low forward voltage". Semicond. Sci. Technol. 35, 125023, (2020).

[7] Tsay, C., et al. "Improving the photoelectrical characteristics of self-powered p-GaN film/n-ZnO nanowires heterojunction ultraviolet photodetectors through gallium and indium co-doping." *Materials Science in Semiconductor Processing*. 121: 105295, (2021).

[8] Liyanage, T., Ahmad, Q., Gymama, S. "Application of nanomaterials for chemical and biological sensors": A review. *IEEE Sensors Journal* 21.11: 12407-12425, (2020).

[9] Terna, D., et al. "The future of semiconductors nanoparticles: Synthesis, properties and applications". *Materials Science and Engineering: B* 272: 115363, (2021).

[10] Meneghini, M., et al. "GaN-based power devices: Physics, reliability, and perspectives". *Journal of Applied Physics* 130.18: 181101, (2021).

[11] Roccaforte, F., Giannazzo, F., Greco, G. "Ion Implantation Doping in Silicon Carbide and Gallium Nitride Electronic Devices". Micro.; 2(1): 23-53, (2022).

[12] Nozaki, M., Terashima, D., Yamada,T., Yoshigoe, A., Hosoi ,T., Shimura, T., et al. "Comparative study on thermal robustness of GaN and AlGaN/GaN MOS devices with thin oxide interlayers". Japanese Journal of Applied Physics. 58(SC): SCCD08, (2019).

[13] Amano, H., et al. "The 2018 GaN power electronics roadmap". *Journal of Physics D: Applied Physics* 51.16: 163001, (2018).

[14] Reshchikov, M., et al. "Stability of the CNHi Complex and the Blue Luminescence Band in GaN". *physica status solidi (b)* 258.12: 2100392, (2021).

[15] Tsao, Y., et al. "Ultrawide-bandgap semiconductors: research opportunities and challenges". *Advanced Electronic Materials* 4.1: 1600501, (2018).

[16] Sierakowski, K., et al. "High pressure processing of ion implanted GaN". *Electronics* 9. 9: 1380, (2020).

[17] Lorenz, K. "Ion Implantation into Nonconventional GaN Structures". *Physics* 4.2: 548-564, (2022).

[18] Uedono, A., et al. "Effect of Ultra-High-Pressure Annealing on Defect Reactions in Ion-Implanted GaN Studied by Positron Annihilation". *physica status solidi (b)* 259.10: 2200183, (2022).

[19] Roccaforte, F., Filippo, G., Giuseppe, G. "Ion Implantation Doping in Silicon Carbide and Gallium Nitride Electronic Devices". *Micro*. 2. 1. MDPI, (2022).

[20] Rebohle, L., et al. "Semiconductor Applications". *Flash Lamp Annealing: From Basics to Applications*: 131-232, (2019).

[21] Hursan, D., Abel, M., Baan, K., Fako, E., Samu, G. F., Nguyen, H. C., et al. "CO_2 Conversion on N-Doped Carbon Catalysts via Thermo- and Electrocatalysis: Role of C–NOx Moieties". ACS Catal., 12(16): 10127, (2022).

[22] Meneghini, M., De Santi, C., Abid, I., Buffolo, M., Cioni, M., Khadar, R. A., et al. "GaN-based power devices: Physics, reliability, and perspectives". Journal of applied physics; 130(18): 181101, (2021).

[23] Ramesh, C., Tyagi, P., Gautam, S., Ojha, S., Gupta, G., Senthil, M., Kushvaha., S. "Controlled growth of GaN nanorods directly on flexible Mo metal foil by laser molecular beam epitaxy". Materials Science in Semiconductor Processing, 111, (2020).

[24] Rodriguez-Benitez, O., et al. "Comparative performance and assessment study of a current-fed dc-dc resonant converter combining si, sic, and GaN-based power semiconductor devices". *Electronics* 9.11: 1982, (2020).

[25] Mohamed, A., Stroscio, M., Mitra, A., Junxia, D., Shi, L. "Transport in III-Nitride Devices Defense Committee". (2019).

[26] Chunduri, K., Schmela., M. "Heterojunction solar technology". *Taiyang News, Munich, Germany*, (2019).

[27] Liu, H., Yin, H., Yang, T., Ding, H., Dong, Y. "Electrogenerated chemiluminescence resonance energy transfer between $ZnGa_2O4$/g-C3 N 4 and gold nanoparticles/graphene and its application in the detection of thrombin". Analyst (London).; 145(22): 7412-20, (2020).

[28] Wang, Y., et al. "Comparative study on dynamic characteristics of GaN HEMT at 300 K and 150 K". IEEE J. Electron Devices Soc, (2020).

[29] Gu, Y., Wang, Y., Chen, J., Chen, B., Wang, M., Zou, X. "Temperature-Dependent Dynamic Degradation of Carbon-Doped GaN HEMTs". TED.; 68(7): 3290-5, (2021).

[30] Ren, Q., Wang, H., Lu, X., Tong, Y., Li, G. "Recent Progress on MOF-Derived Heteroatom-Doped Carbon-Based Electrocatalysts for Oxygen Reduction Reaction". Advanced Science; 5(3): 1700515, (2018).

[31] Zhang, Y., Chen, Z., Zhang, K., Feng, Zhao, H. "Laser-Assisted Metal–Organic Chemical Vapor Deposition of Gallium Nitride". Phys Status Solidi RRL.; 15(6), (2021).

[32] You, S., Geens, K., Borga, M., Liang, H., Hahn, H., Fahle, D., et al. "Vertical GaN devices: Process and reliability. Microelectronics and reliability". 126: 114218, (2021).

[33] Di Pede, E., Roland, M. "Preghiera e filiazione nel Vangelo di Luca (coll. Epifania della Parola. Testi ermeneutici, 12)", Revue theologique de Louvain. 2012;43(4):587-8, (2010).

[34] Loeto, K. "Uncovering the carrier dynamics of AlInGaN semiconductors using time-resolved cathodoluminescence". Materials science and technology. 38(12): 780-93, (2022).

[35] Gao, Y., Sun, D., Jiang, X., Zhao, J. "Point defects in group III nitrides: A comparative first-principles study". Journal of applied physics. 125(21): 215705, (2019).

[36] Nahhas, A. M. "Review of GaN Nanowires Based Sensors. American journal of nanomaterials". 8(1): 32-47, (2020).

[37] Zhang, M., Zhao, C., Gong, H., Niu, G., Wang, F. "Porous GaN Submicron Rods for Gas Sensor with High Sensitivity and Excellent Stability at High Temperature". ACS Appl. Mater. Interfaces, 11, 33124-33131, (2019).

[38] Shi, C., Rani, A., Thomson, B., Debnath, R., Motayed, A., Yoannou, D.E., Li, Q. "High-performance room-temperature TiO_2 -functionalized GaN nanowire gas sensors". Appl. Phys. Lett. 115, 121602, (2019).

[39] Zhang, M., Zhao, C., Gong, H., Niu, G., Wang, F. "High Sensitivity Gas Sensor Based on Porous GaN Nanorods with Excellent High-Temperature Stability". In Proceedings of the 2019 20th International Conference on Solid-State Sensors, Actuators and Microsystems & Eurosensors XXXIII (TRANSDUCERS & EUROSENSORS XXXIII), Berlin, Germany, pp. 1369-1372, (2019).

[40] Gomes, B. A., Rodrigues, J., Rabelo, R., Kumar, N., Kozlov, S. "IoT-Enabled Gas Sensors: Technologies, Applications, and Opportunities". JSAN, 8, 57, (2019).

[41] Khan, M., Thomson, B., Motayed, A., Li, Q., Rao, M. "Functionalization of GaN Nanowire Sensors with Metal Oxides: An Experimental and DFT Investigation". IEEE Sens. J., 99, 1, (2020).

[42] Chen, F., Xiaohong, J., Shu, L. "Recent progress in group III-nitride nanostructures: From materials to applications". *Materials Science and Engineering: R: Reports* 142: 100578, (2020).

[43] Mengwei, S., et al. "Characterization and simulation of 280 nm UV-LED degradation." *AIP Advances* 11.3 (2021): 035315. Despaigne et al., "Full InGaN red light emitting diodes", *J. Appl. Phys.*, 128, (2020).

[44] Dussaigne, A., et al. "Full InGaN red (625 nm) micro-LED (10 μ m) demonstration on a relaxed pseudo-substrate". *Appl. Phys. Exp.*, 14, 9, (2021).

[45] Zhuang, Z., Iida D., Ohkawa, K. "Investigation of InGaN-based red/green micro-light-emitting diodes", *Opt. Lett.*, 46, 8, 1912-1915, (2021).

[46] Oh, J., et al. "Light output performance of red AlGaInP-based light emitting diodes with different chip geometries and structures", *Opt. Exp.*, 26, 9, 11194-11200, (2018).

[47] Iida, D., Zhuang, Z., Kirilenko, P., Velazquez-Rizo M., Ohkawa, K. "Demonstration of low forward voltage InGaN-based red LEDs", *Appl. Phys. Exp.*, 13, 3, (2020).

[48] Iida, D., Zhuang, Z., Kirilenko, P., Velazquez-Rizo, M., Najmi M., Ohkawa, K. "633-nm InGaN-based red LEDs grown on thick underlying GaN layers with reduced in-plane residual stress". *Appl. Phys. Lett.*, 116, 16, (2020).

[49] Wang, X., Kumagai, N., Hao, G. "High-efficiency high-power AlGaInP thin-film LEDs with micron-sized truncated cones as light-extraction structures". *Phys. Status Solidi (A)*, 215, 6, (2018).

[50] Chen, S., et al. "Full-color monolithic hybrid quantum dot nanoring micro light-emitting diodes with improved efficiency using atomic layer deposition and nonradiative resonant energy transfer", *Photon. Res.*, 7, 4, 416-422, (2019).

[51] Smith, J., et al. "Comparison of size-dependent characteristics of blue and green InGaN microLEDs down to 1 μ m in diameter", *Appl. Phys. Lett.*, 116, 7, (2020).

[52] Guo, J., Ding, J., Mo, C., Zheng, C., Jiang, F. "Effect of AlGaN interlayer on luminous efficiency and reliability of GaN-based green LEDs on silicon substrate". *Chin. Phys. B*, 29, 4, (2020).

[53] Pasayat, S., et al. "Demonstration ultra-small (<10 μ m) 632 nm red InGaN micro-LEDs with useful on-wafer external quantum efficiency (>0.2%) for mini-displays". *Appl. Phys. Exp.*, 14, (2021).

[54] Zhang, S., Zhang, J., Gao, X., Wang, C., Zheng, M., et al. "Efficient emission of InGaN-based light-emitting diodes: Toward orange and red". *Photon. Res.*, 8, 11, 1671-1675, (2020).

[55] Bai, J., et al. "Ultrasmall ultracompact and ultrahigh efficient InGaN micro light emitting diodes (μ LEDs) with narrow spectral line width). *ACS Nano*, 14, 6, 6906-6911, (2020).

[56] Amador-Mendez, N. "Nanostructured III-nitride light emitting diodes. Micro and nanotechnologies/Microelectronics". Universite Paris-Saclay, (2022).

[57] Li, P., et al. "Very high external quantum efficiency and wall-plug efficiency 527 nm InGaN green LEDs by MOCVD". *Opt. Exp.*, 26, 25, 33108-33115, (2018).

[58] Sarkar, B., et al. "N-and P-type doping in Al-rich AlGaN and AlN". *ECS Trans.*, 86, 12, 25, (2018).

[59] Pasayat, S., et al. "Demonstration of ultra-small (< 10 μ m) 632 nm red InGaN micro-LEDs with useful on-wafer external quantum efficiency (> 0.2%) for mini-displays", *Appl. Phys. Exp.*, 14, 1, (2020).

[60] Wong, M., et al. "Improved performance of AlGaInP red micro-light-emitting diodes with sidewall treatments", *Opt. Exp.*, 28, 4, 5787-5793, (2020).

[61] Maity, A., Grenadier, S., Li, J., Lin, J., Jiang, H. X. "Hexagonal boron nitride: Epitaxial growth and device applications", Progress in Quantum Electronics, 76,100302, ISSN 0079-672., (2021).

[62] Maity, S., Grenadier, J., Li, J., Lin, H., Jiang, Y., et al. "Hexagonal Boron Nitride on III–V Compounds: A Review of the Synthesis and Applications". Materials 15.13, (2022).

[63] Ng, T. K., Holguin-Lerma, J. A., Kang, C. H., Ashry, I., Zhang, H., Bucci, G., & Ooi, B. S. "Group-III-nitride and halide-perovskite semiconductor gain media for amplified spontaneous emission and lasing applications." Journal of Physics D: Applied Physics 54.14, 143001, (2021).

[64] Pandey, J., Gim, R., Hovden, Z. "An AlGaN tunnel junction light emitting diode operating at 255 nm". *Appl. Phys. Lett.*, 117, 24, (2020).

[65] Pandey, J., Gim, R., Hovden Z. "Electron overflow of AlGaN deep ultraviolet light emitting diodes". *Appl. Phys. Lett.*, 118, 24, (2021).

[66] Liang, Y., Towe, E. "Progress in efficient doping of high aluminum-containing group III-nitrides", *Appl. Phys. Rev.*, 5, 1, (2018).

[67] Lu, W., et al. "Colour-tunable emission in coaxial GaInN/GaN multiple quantum shells grown on three-dimensional nanostructures". *Applied Surface Science* 539:148279, (2021).

[68] Zhang, Z., et al. "A 271.8 nm deep-ultraviolet laser diode for room temperature operation". *Appl. Phys. Exp.*, 12, 12, (2019).

[69] Sato, K., et al. "Room-temperature operation of AlGaN ultraviolet-B laser diode at 298 nm on lattice-relaxed Al 0.6 Ga 0.4 N/AlN/sapphir". *Appl. Phys. Exp.*, 13, 3, (2020).

[70] Tanaka, S., et al. "Effect of dislocation density on optical gain and internal loss of AlGaN-based ultraviolet-B band lasers". *Appl. Phys. Exp.*, 13, 4, (2020).

[71] Mehnke, F., et al. "Electrical and optical characteristics of highly transparent MOVPE-grown AlGaN-based tunnel heterojunction LEDs emitting at 232 nm". *Photon. Res.*, 9, 6, 1117-1123, (2021).

[72] Ruterana, P., Morales, M., Chery, N., Ngo, T., Chauvat, M., Lekhal K., et al. "Effect of AlGaN interlayer on the GaN/InGaN/GaN/AlGaN multi-quantum wells structural properties toward red light emission". Journal of Applied Physics.; 128-22, (2020).

[73] Meier, J., Gerd, B. "Progress and Challenges of InGaN/GaN-Based Core–Shell Microrod LEDs". *Materials* 15.5: 1626. 74, (2022).

[74] Ding, K., Avrutin, O, Morkoc, H. "Status of growth of group III-nitride heterostructures for deep ultraviolet light-emitting diodes", *Crystals*, 7, 10, 300, (2017).

[75] Alfaraj, N., et al. "Deep-ultraviolet integrated photonic and optoelectronic devices: A prospect of the hybridization of group III–nitrides, III–oxides, and two-dimensional materials". *Journal of Semiconductors* 40.12: 121801, (2019).

[76] Yong-Ho, Ra, Cheul-Ro, L. "Core–Shell Tunnel Junction Nanowire-White-Light-Emitting-Diode. *Nano Letters*. *20* (6), 4162-4168, (2020).

[77] Pandey, A., et al. "Enhanced doping efficiency of ultrawide band gap semiconductors by metal-semiconductor junction assisted epitaxy". *Phys. Rev. Mater.*, 3, 5, (2019).

[78] Yang, D., et al. "Self-contained InGaN/GaN micro-crystal arrays as individually addressable multi-color emitting pixels on a deformable substrate". *Journal of Alloys and Compounds* 803: 826-833, (2019).

[79] Chen, F., Xiaohong, J., Shu, P. "Recent progress in group III-nitride nanostructures: From materials to applications". Materials Science and Engineering: R: Reports, Volume 142,100578, ISSN 0927-796X, (2020).

[80] Janjua, B., Sun, H., Zhao, C., Anjum, D., Wu, F., Alhamoud, A., et al. "Self-planarized quantum-disks-in-nanowires ultraviolet-B emitters utilizing pendeo-epitaxy. Nanoscale. 2017 Jun 14; 9(23): 785-7813, (2017).

[81] Sergent, S., Damilano, B., Vezian, S., Chenot, S., Tsuchizawa, T., Notomi, M. "Lasing up to 380 K in a sublimated GaN nanowire". *Appl. Phys. Lett*, (2020).

[82] Priante, D. "*Study of ultraviolet AlGaN nanowires light-emitting diodes*". Diss, (2019).

[83] Moab, P., Dipayan, D., Mehrdad, D., Md, B., Thang H., Durgamadhab, M., Abdallah, K., James, P., Hoang, N., Khai, Hieu, T, "Fabrication of Phosphor-Free III-Nitride Nanowire Light-Emitting Diodes on Metal Substrates for Flexible Photonics". *ACS Omega*, *2* (9), 5708-5714, (2017).

[84] Wei, Z., et al. "Micro-LEDs Illuminate Visible Light Communication", in *IEEE Communications Magazine*, (2019).

[85] Robin, Y., Bae, S., Shubina, T., Pristovsek, M., Evropeitsev, E., Kirilenko, D., Davydov, V., Smirnov, A., Toropov, A., Jmerik, V., Kushimoto, M., Nitta, S., Ivanov, S., Amano, H. "Insight into the performance of multi-color InGaN/GaN nanorod light emitting diodes". Sci Rep. 9; 8(1): 7311, (2018).

[86] Hartensveld, M., Ouin, G., Liu, C., Zhang, J. "Effect of KOH passivation for top-down fabricated InGaN nanowire light emitting diodes". *J. Appl. Phys.*, 126, 18, (2019).

[87] Zhao, S., Wang, R., Chu, S., Mi, Z. "Molecular Beam Epitaxy of III-Nitride Nanowires: Emerging Applications from Deep-Ultraviolet Light Emitters and Micro-LEDs to Artificial Photosynthesis". 13, 2, 6-16, (2019).

[88] Wu, T., et al. "Mini-LED and micro-LED: Promising candidates for the next generation display technology". *Appl. Sci.*, 8, 9, 1557, (2018).

[89] Wasisto, H., Prades, J., Gulink, J., Waag, A. "Beyond solid-state lighting: Miniaturization, hybrid integration, and applications of GaN nano- and micro-LEDs". Applied Physics Reviews.;6(4), (2019).

[90] Jiang, H., Jingyu, L. "Development of nitride microLEDs and displays". *Semiconductors and Semimetals*. Vol. 106. Elsevier, 1-56, (2021).

[91] Zou, X., et al. "GaN Single Nanowire p–i–n Diode for High-Temperature Operations". ACS Applied Electronic Materials 2.3: 719-724, (2020).

[92] Yin, H., et al. "The recent advances in C60 micro/nanostructures and their optoelectronic applications". Organic Electronics 93: 106142. (2021).

[93] Subramani, S., Kulandaivel, J. "Ultrasensitive Self-powered Heterojunction Ultraviolet Photodetector of p-GaN Nanowires on Si by Halide Chemical Vapour Deposition. Nanotechnology, 34, 13, (2022).

[94] Sett, S., Arup, K. R. "Effective Separation of Photogenerated Electron-Hole Pairs by Radial Field Facilitates Ultrahigh Photoresponse in Single Semiconductor Nanowire Photodetectors". The Journal of Physical Chemistry C 124.41: 22808-22816, (2020).

[95] Larkin, I. A., Vdovin, E., Yu, N. "Theoretical model of giant oscillations of the photocurrent in GaAs/AlAs pin diodes". Physica Scripta 97.9: 095811, (2022).

[96] Johar, M., et al. "Universal and scalable route to fabricate GaN nanowire-based LED on amorphous substrate by MOCVD". Applied Materials Today 19: 100541, (2020).

[97] Goswami, L., et al. "Graphene quantum dot-sensitized ZnO-nanorod/GaN-nanotower heterostructure-based high-performance UV photodetectors". ACS applied materials & interfaces 12.41: 47038-47047, (2020).

[98] Wu, Y. "*III-Nitride Nanocrystal Based Green and Ultraviolet Optoelectronics"*. Diss, (2020).

[99] Liu, X., Ayush P., Zetian M. "Nanoscale and quantum engineering of III-nitride heterostructures for high efficiency UV-C and far UV-C optoelectronics". *Japanese Journal of Applied Physics.* 60. 11: 110501. (2021).

[100] Concordel, A., et al. "The role of surface states and point defects on optical properties of InGaN/GaN multi-quantum wells in nanowires grown by molecular beam epitaxy". *Nanotechnology* 34.3: 035703, (2022).

[101] Subramani, S., Kulandaivel, J. "Ultrasensitive Self-powered Heterojunction Ultraviolet Photodetector of p-GaN Nanowires on Si by Halide Chemical Vapour Deposition". *Nanotechnology*, (2022).

[102] Alavi, K., et al. "Photodetection Using Atomically Precise Graphene Nanoribbons". *ACS Applied Nano Materials* 3.8: 8343-8351, (2020).

[103] Kim, J., et al. "Designing an Ultrathin Film Spectrometer Based on III-Nitride Light-Absorbing Nanostructures". *Micromachines* 12.7: 760, (2021).

[104] Jegannathan, G., et al. "An overview of cmos photodetectors utilizing current-assistance for swift and efficient photo-carrier detection". *Sensors* 21.13: 4576. (2021).

[105] Aiello, A., et al. "Deep ultraviolet monolayer GaN/AlN disk-in-nanowire array photodiode on silicon". *Applied Physics Letters* 116. 6: 061104, (2020).

[106] Yang, H. "An Introduction to Ultraviolet Detectors Based on III Group-Nitride Semiconductor". *Journal of Physics: Conference Series*. 1676. 1. IOP Publishing, (2020).

[107] Kaur, D., Mukesh, K. "A strategic review on gallium oxide based deep-ultraviolet photodetectors: recent progress and future prospects". *Advanced optical materials* 9.9: 2002160, (2021).

[108] Liu, J., et al. "Organic and quantum dot hybrid photodetectors: towards full-band and fast detection". *Chemical Communications*, (2023).

[109] Shen, L., Edwin P., Johnny, H. "Recent developments in III–V semiconducting nanowires for high-performance photodetectors". *Materials Chemistry Frontiers* 1.4: 630-645, (2017).

[110] Spies, M., Eva, M. "Nanowire photodetectors based on wurtzite semiconductor heterostructures". *Semiconductor Science and Technology* 34.5: 053002, (2019).

[111] Aggarwal, N., Shibin, K., Govind, G. "GaN Nanoflowers: Growth to Optoelectronic Device". *21st Century Nanoscience–A Handbook*: 8-1, (2020).

[112] Sarkar, K., et al. "III-V nanowire-based ultraviolet to terahertz photodetectors: Device strategies, recent developments, and future possibilities". *TrAC Trends in Analytical Chemistry* 130: 115989, (2020).